A simple analysis of an inductive RF discharge

R B Piejak, V A Godyak and B M Alexandrovich
GTE Laboratories Inc, 40 Sylvan Road, Waltham, MA 02254, USA

Received 15 May 1992, in final form 17 July 1992

Abstract. The electrical properties of an inductive low pressure RF discharge have been analysed by considering the discharge to be a one-turn secondary of an air-core transformer. Expressions for spatially averaged quantities representing familiar discharge parameters such as the voltage, current and electric field have been determined as functions of measured electrical parameters of the primary circuit. Based on an analytical expression relating the coupling between the electrical characteristics of the primary coil and the plasma load, scaling laws for plasma parameters and the RF power distribution between the inductor coil and the discharge have been determined. The analysis developed here was applied to a collisionally dominated inductive RF discharge in a mercury–rare gas mixture. It may also be applied as a practical design and optimization tool for a plasma processing source based on an inductive discharge.

1. Introduction

Inductively coupled (electrodeless) discharges hold much promise as plasma sources for electrical discharge lighting and plasma processing. Since they do not depend upon large voltages to drive displacement current through the powered RF sheaths, ion energies in inductive discharges are considerably lower than those found in capacitively coupled RF discharges (especially at high power density). Relatively low ion energies in inductive discharges result in a decrease in ion–wall interactions (e.g. sputtering, etching and a variety of energetic ion-induced chemical reactions). In many instances, inductively coupled discharges efficiently provide a high density plasma with relatively small ion power loss in the sheaths. Moreover, plasma generation and ion acceleration processes can be independently controlled for inductive discharges in plasma processing reactors through RF biasing of the remote substrate, resulting in independent control of the ion energy.

Inductively coupled discharges have been known for over a century [1, 2] and many authors have analysed their operation. A short concise literature review dealing with modelling low-pressure, collisional discharges maintained by an RF current applied to an induction coil is contained in recent papers by Lister and Cox [3] and by Denneman [4]. In these works the spatial distribution of the plasma RF field and the current density are numerically calculated by solving a coupled set of Maxwell equations for an internal (referenced to the plasma) [3] and an external [4] inductor coil. Assuming diffusion-controlled plasma density profiles (one with zero boundary values) for cylindrical and coaxial plasmas and collisional RF power transfer to electrons, the authors [3, 4] were able to couple electrical parameters at the primary coil with given plasma parameters for discrete (measurement) points. Such analyses of a real experiment are somewhat qualitative in nature because of the assumptions mentioned above and also because a one-dimensional model was assumed. Note that generally, in applications, the inductor coil length is comparable to (or even shorter than) the plasma dimension and the coil diameter.

In this work, as in previous works, a low-pressure inductive RF discharge is studied by considering it to be the secondary of an air-core transformer. However, numerical solutions of Maxwell equations and most of the underlying assumptions about the plasma density distribution and the mechanism of RF power dissipation needed to solve these equations are avoided by taking advantage of well known electrical circuit principles (which follow from Maxwell's equations) governing air-core transformers and solenoidal inductors. In the present approach only integral plasma parameters are considered (such as discharge current, voltage and power) regardless of their particular spatial distributions. The spatial distribution is formally accounted for through the coupling coefficient between the primary coil and the plasma which can be determined from experiment. An integral representation of plasma parameters, rather than the differential representation given in [3, 4], is quite advantageous since it considerably simplifies the analysis and enables one to generate analytical formulae for the relationships between external electrical and plasma characteristics. Furthermore, since the spatial discharge characteristics are not essential to this analysis,

the relationships obtained here can be applied to different inductive discharge configurations such as external, internal and immersed inductor coils of finite length, without knowledge of the particular mechanisms involved in forming the plasma density profile and in RF power transfer.

In the experimental part of this work the external electrical characteristics of inductive discharges in a mercury–rare gas mixture (typical for a fluorescent lamp) were measured over a range of discharge power, and internal plasma parameters were inferred from analytical formulae obtained here. It is assuring to note that as a function of discharge current the plasma parameters determined in this way appear to have general characteristics that are similar to those possessed by all low pressure gas discharges (DC, low frequency and capacitively coupled RF). For example, over a wide range of discharge current the plasma electric field is almost constant, thereby resulting in a plasma density that is proportional to the discharge current and RF power.

2. Transformer formalism

To model a low-pressure inductively coupled discharge, the discharge is regarded as the secondary coil of an air-core transformer as shown in figure 1. The primary of the transformer is the induction coil itself, which is composed of n turns with values of inductance L_0 and resistance R_0 (or Q-factor, $Q = \omega L_0/R_0$) that are measured beforehand. A sinusoidal RF voltage with an RMS value V_1 and radian frequency ω is applied to the primary coil resulting in a primary coil current I_1. Since the discharge is an electrically conductive fluid that surrounds the coil, it is considered to be a multitude of filamentary discharges that essentially run in parallel, forming, in practice, a one turn secondary winding of an air-core transformer with an inductance L_2' and a plasma resistance R_2.

The discharge inductance L_2' consists of two components: the electron inertia inductance L_e, which follows from the plasma conductivity formula $\sigma = e^2 n_e/m(\nu + j\omega)$, where e is electron charge, m is electron mass, n_e is plasma density and ν is the effective electron collision frequency, and the geometric (or magnetic) inductance L_2, which is due to the discharge current path. L_2 is inductively coupled to the primary coil through mutual

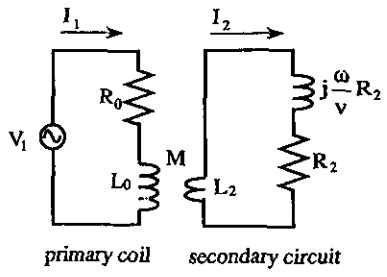

Figure 1. Electrical circuit representation of an inductive RF discharge as the secondary of an air-core transformer.

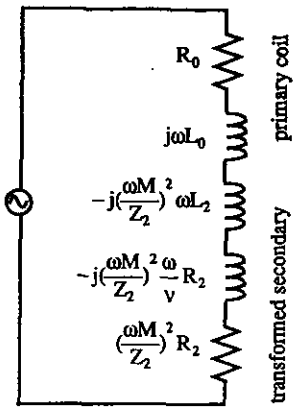

Figure 2. Equivalent circuit of an inductively coupled discharge where the secondary circuit has been transformed into its series equivalent in terms of the primary circuit current.

inductance M while L_e is considered to be the imaginary part of the plasma load impedance, $L_e = R_2/\nu$.

In the analysis presented here it is assumed that the discharge is in a purely inductive mode, implying that the capacitive mode of operation, which appears to dominate upon discharge initiation and at relatively low power, can be ignored and the power transfer to the plasma electrons can be represented by the plasma conductivity formula.

Inductive discharges are generally initiated in a capacitive mode between adjacent turns of a coil to which voltage is applied. When the coil current is large enough to induce an azimuthal RF field that can maintain the ionization process, a clearly visible increase in discharge light intensity occurs and the main mechanism driving the discharge shifts from a capacitive to an inductive mode. For a driving frequency where the wavelength is much larger than the discharge dimensions, the magnetic induction is in phase with the current and the EMF is in phase at all points occupied by the plasma.

The coupled circuits shown in figure 1 can be transformed through a straightforward circuit analysis into that shown in figure 2 using the classic approach given by Termin [5]. In this representation the secondary circuit elements are written in terms of the primary circuit current. From the point of view of the primary circuit, the effect of the coupled secondary circuit is to add the impedance $(\omega M)^2/Z_2$ to the primary circuit, where Z_2 is the complex (vector) impedance of the secondary circuit. With the coupled secondary impedance separated into real and imaginary parts, the equivalent resistance of the primary R_1 is simply the sum of the resistance of the primary coil R_0 and a term representing the coupled secondary resistance R_2, and it may be written as

$$R_1 = R_0 + \omega^2 k^2 L_0 L_2 R_2 / Z_2^2 \qquad (1)$$

where $M^2 = k^2 L_0 L_2$, $Z_2^2 = [\omega L_2 + (\omega/\nu)R_2]^2 + R_2^2$ and k is the coupling coefficient. The equivalent inductance L_1 is of the same general form as R_1 and is the sum of the inductance of the primary and a negative inductance

term representing the total reactance of the coupled secondary. L_1 may be written as

$$L_1 = L_0 - \omega k^2 L_0 L_2[\omega L_2 + (\omega/\nu)R_2]/Z_2^2. \quad (2)$$

The negative sign associated with the secondary reactance can be simply understood by noting that current in the secondary causes some of the magnetic flux in the primary to be neutralized, thus resulting in a lower total magnetic flux in the primary circuit [5].

Note that in an ideal transformer the coupling is perfect ($k = 1$) and $(\omega M/Z)^2 = n^2$, and the secondary inductance is $L_2 = L_0/n^2$. Thus, for an ideal transformer, the inductive reactance of the secondary totally offsets the reactance of the primary and the resulting equivalent primary circuit is purely resistive ($R_1 = R_2 n^2$). In general, the coupling of an air-core transformer is not perfect and $(\omega M/Z)^2 \neq n^2$.

Equations (1) and (2) are independent equations containing three unknown quantities (R_2, L_2 and k). A third equation (needed for an analytical solution) follows directly from the basic premise of this work: that the plasma is a one-turn current path that surrounds the primary coil and can be considered as a secondary of an air-core transformer. Since the primary coil is surrounded by a conductive fluid (the plasma) and makes a closed electrical path about the primary coil, the premise of a single-turn secondary appears entirely reasonable. To take advantage of this premise it must be recalled that the inductance L_s of a solenoid, with $h_s \geqslant r_s$, is proportional to $n_s^2 r_s^2$, where n_s, h_s and r_s are the number of turns, the length and the radius of the solenoid respectively. Thus, $L_0 \propto n^2 r_0^2$ and $L_2 \propto r^2$, where r_0 is the radius of the primary coil, r is the equivalent radius of the discharge path and $n_s = 1$ for L_2. Assuming the lengths of inductors L_0 and L_2 to be equal, we can write

$$L_2 = L_0 r^2/(n^2 r_0^2).$$

For equal length coaxially oriented inductors $k \approx r_0^2/r^2$ for $r > r_0$ and $k \approx r^2/r_0^2$ for $r < r_0$. In what follows, corresponding to the geometry of our experiment, we will consider the case $r > r_0$, although this analysis is equally applicable to either case. Thus, the discharge inductance can be written as

$$L_2 = L_0/kn^2. \quad (3)$$

Equations (1), (2) and (3) can now be solved analytically thus coupling the electrical characteristics of the primary coil with the electrical characteristics of the plasma load:

$$k^2 = [\omega^2(L_0 - L_1)^2 + (R_1 - R_0)^2]/\omega L_0[\omega(L_0 - L_1) - \omega/\nu(R_1 - R_0)] \quad (4)$$

$$R_2 = (\omega L_0/kn^2)(R_1 - R_0)/[(\omega(L_0 - L_1) - \omega/\nu(R_1 - R_0)] \quad (5)$$

$$I_2 = I_1 \omega L_0(\sqrt{k}/n)[(\omega L_0/kn^2 + R_2\omega/\nu)^2 + R_2^2]^{-1/2} \quad (6)$$

$$V_p = I_2 R_2 \quad (7)$$

$$P_d = V_p^2/R_2 \quad (8)$$

where I_2 is the RMS discharge current, V_p is the ohmic part of the plasma voltage (in phase with the plasma current) and P_d is the RF power dissipated in the discharge.

3. Plasma parameter evaluation

Using the relationships determined in equations (4)–(8) one can evaluate the electrical characteristics of the plasma load and find some integral and spatially averaged discharge parameters through given experimental constants L_0, Q, r_0, ω and ν and a measured set of electrical parameters such as L_1, R_1 and P or I/V and the phase characteristics of the primary coil. These measureable parameters are coupled through the simple expressions:

$$P = I_1 V_1 \cos\varphi \qquad R_1 = \cos\varphi V_1/I_1$$
$$L_1 = \sin\varphi V_1/\omega I_1.$$

Having inferred the values of the plasma voltage V_p and coupling coefficient k one can readily evaluate the effective plasma RF field along the discharge path averaged across a zone where the current is localized (about radius r):

$$E_r = V_p/2\pi r = V_p\sqrt{k}/2\pi r_0. \quad (9)$$

Note that $E_r = E_p(1 + \omega^2/\nu^2)^{-1/2}$ where E_p is the RMS value of the RF electric field in the plasma at radius r.

After evaluating E_r, the total number of electrons N_e, the averaged plasma density $\langle n_e \rangle$, the averaged plasma conductivity $\langle \sigma_0 \rangle = e^2 < n_e > /m\nu$ and the skin depth $\langle \delta \rangle$ can be estimated from a power balance equation:

$$P_d = \int (e^2 n_e/m\nu)E^2 \, dA = (e^2/m\nu) < E^2 > N_e$$
$$= (e^2/m\nu)cE_r^2 N_e \quad (10)$$

$$c = \langle E^2 \rangle / E_r^2 \quad (11)$$

$$N_e = P_d m\nu/ce^2 E_r^2 \quad (12)$$

$$\langle n_e \rangle = P_d m\nu/ce^2 E_r^2 A \quad (13)$$

$$\langle \sigma_0 \rangle = P_d/cAE_r^2 \quad (14)$$

$$\langle \delta \rangle = E_r(2cA/\omega\mu_0 P_d)^{1/2} \quad (15)$$

where E is the effective local RF field in the plasma, c is a form factor accounting for the difference between E_r^2 and $\langle E^2 \rangle$ which is averaged over the entire plasma volume, A is the plasma volume and μ_0 is the vacuum magnetic permeability. Form-factor c depends on the radial and axial distributions of the plasma density and the local RF field. Although in this form both plasma conductivity and skin depth appear to depend on discharge power density P_d/A, regardless of the particular value of ν and consequently gas pressure p, gas pressure indirectly influences the inferred values $\langle \sigma_0 \rangle$ and $\langle \delta \rangle$ through the dependence of E_r on p.

4. Power transfer efficiency and minimum maintenance power

The power transfer efficiency ξ, defined as the ratio of the RF discharge power P_d to total RF power P needed to maintain an inductive discharge, is an especially important parameter for applications where energy efficiency is desirable. The total power P consists of two parts: $P = P_d + P_t$, where P_t is the power dissipated in the primary coil. Thus, $\xi = P_d/P = [1 + P_t/P_d]^{-1}$. The ratio P_t/P_d (see figure 2) can be written as

$$P_t/P_d = R_0/(R_1 - R_0) = (R_2 k^2 Q \omega L_2)^{-1}[(\omega L_2 + (\omega/\nu)R_2)^2 + R_2^2] \quad (16)$$

A more convenient representation of P_t/P_d is in terms of experimental constants L_0, Q and n and measureable parameters P_d, V_p and k, since (as will be shown in the experimental section) the last two are essentially constant over a wide range of power:

$$P_t/P_d = n^2 P_d (kQ\omega L_0 V_p^2)^{-1}[(\omega L_0/kn^2 + (\omega/\nu)V_p^2/P_d)^2 + V_p^4/P_d^2]. \quad (17)$$

From this representation the qualitative behaviour at the extremes of the discharge power can be readily understood with little knowledge of the actual discharge parameters. With the normalization $t = k^2 Q P_t/P_d$ and $Y = X_2/R_2 = (\omega L_0/kn^2)(P_d/V_p^2)$, equation (17) can be written as

$$t = Y^{-1}[(Y + \omega/\nu)^2 + 1]. \quad (18)$$

In this form P_t/P_d can be easily visualized as shown in figure 3.

It follows from equation (17) and figure 3 that, for decreasing discharge power when $Y \ll \omega/\nu$, $t \approx (\omega^2/\nu^2 + 1)Y^{-1}$, the ratio $P_d/P_t \to 0$ and $\xi \to 0$ while $P_t \approx P_{min}$ approaches some minimal value P_{min} given by

$$P_{min} = n^2 V_p^2 (kQ\omega L_0)^{-1}(1 + \omega^2/\nu^2). \quad (19)$$

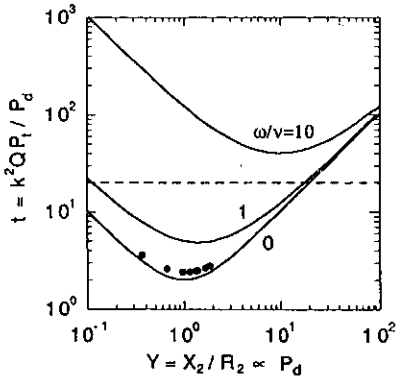

Figure 3. A normalized ratio P_t/P_d shown as a function of $Y = X_2/R_2$ for $\omega/\nu = 0$, 1 and 10. The discrete points shown in the figure are based on experimental data with $\omega/\nu = 0.18$ and indicate the range of the experimental data in terms of Y. The broken line represents a boundary between efficient ($\xi > 0.5$) and inefficient ($\xi < 0.5$) power transfer at $k^2Q = 20$.

P_{min} represents the power loss in the primary coil needed to create a circular RF field equal to the plasma RF field but with no plasma present ($P_d = 0$). Below this value of RF power an inductive steady-state discharge is impossible to maintain. The existence of a minimal maintenance power is fundamental to all inductive discharges and directly follows from Maxwell's equations and the ionization and energy balance in a weakly ionized gas. Indeed, to sustain an inductive plasma, an electric field must be created around a closed path with a magnitude that satisfies the ionization and electron energy balances. This electric field is induced by the primary RF current which dissipates energy due to the resistance of the primary coil.

Noting that the inductance of a cylindrical coil with length h can be written as:

$$L_0 = n^2 \pi r_0^2 \mu_0/h(1 + 0.88 r_0/h) \quad (20)$$

one obtains

$$P_{min} = 10^7 h E_r^2 (1 + 0.88 r_0/h)(1 + \omega^2/\nu^2)/\omega k^2 Q \quad (21)$$

with units $P_{min}(W)$, $E_r(V/m)$, $h(m)$ and $r_0(m)$.

In the opposite limit of large discharge power and large plasma conductivity, $t \approx Y$ and $P_d/P_t \to 0$ while $P \approx P_t$ grows quadratically with discharge power:

$$P_{max} = YP_d/k^2 Q = P_d^2 \omega L_0/k^3 n^2 Q V_p^2 \quad (22)$$

which corresponds to the limit of infinite conductivity in the secondary (plasma) circuit with inefficient power transfer to the plasma ($\xi \to 0$).

Note that the limiting cases of small and large discharge power considered here correspond (and have a profound analogy) to the well known property of an ordinary transformer with an open and with a shorted secondary winding respectively. In both cases no power is dissipated in the load but in both cases there is power dissipated in the primary winding due to inherent resistive losses in the winding itself.

Between the two extremes there is a point of maximum power transfer efficiency which occurs when

$$X_2 = \omega L_0/kn^2 = V_p^2(1 + \omega^2/\nu^2)^{1/2}/P_d = |Z_p| \quad (23)$$

which corresponds to an equality between the secondary reactance X_2 and the plasma impedance $|Z_p|$. At this point the ratio P_t/P_d is minimal which corresponds to maximal possible power transfer efficiency,

$$(P_t/P_d)_{min} = 2[(1 + \omega^2/\nu^2)^{1/2} + \omega/\nu]/k^2 Q. \quad (24)$$

At the low frequency limit ($\omega/\nu \ll 1$) which is typical for a fluorescent lamp having a gas pressure around 1 Torr and at a driving frequency of 13.56 MHz

$$(P_t/P_d)_{1,min} = 2/k^2 Q \quad (25)$$

while at the high-frequency limit ($\omega^2/\nu^2 \gg 1$),

$$(P_t/P_d)_{h,min} = 4(\omega/\nu)/k^2 Q \gg (P_t/P_d)_{1,min}. \quad (26)$$

The increase in coil loss at large ω/ν is due to a rise in the RF field in the plasma E_p (and also in the primary current) needed to maintain the RF discharge. It should be remembered that $E_p = E_r(1 + \omega^2/\nu^2)^{1/2}$ and E_r remains

nearly constant for a given discharge geometry and gas pressure independent of frequency. The coil loss can be a significant (or even dominant) portion of the total RF power delivered to an inductively coupled RF plasma source; this may be the case in low pressure (around a mTorr) inductive discharges with $\omega^2/\nu^2 \gg 1$. In any case, the issue of coil loss should be properly addressed when determining the RF power dissipated in the plasma from the measurement of total RF power.

From equation (17) and figure 3 one can find the conditions at which energy transfer into an inductive RF discharge is inefficient. Assuming the criterion for efficient operation to be $P_t/P_d \leqslant 1$ which corresponds to $\xi \geqslant 0.5$, one can see in figure 3 that, for a given ω/ν and device parameters k^2Q (ranging in real devices somewhere between 5 and 100), there is only a limited range of discharge power (Y-parameter) where efficient operation is possible. In figure 3 this is shown for $k^2Q = 20$ and $\omega/\nu = 1$, where efficient operation is achieved for Y between 0.1 and 20. For $\omega/\nu = 10$, efficient operation is impossible (no crossing between the line of $k_2Q = 20$ and $t(Y)$). For this last case, according to equation (26), $(P_t/P_d)_{min} = 2$ and maximal efficiency $\xi = 1/3$ only for a single point $Y = 10$.

5. Experimental results and discussion

This experiment was carried out in an inductively coupled RF discharge in a Hg–rare gas mixture typical for a fluorescent lamp discharge and corresponding to $\omega/\nu \approx 0.18$. The discharge was contained by a glass vessel with a spherical external shape having an outer diameter of 10 cm. A partial cross-sectional view of the discharge configuration is shown in figure 4. A cylindrical reentrant cavity with a 3.6 cm inner diameter enclosed the primary coil, thus the discharge surrounded the primary coil but was not in direct contact with it. The primary coil was composed of seven turns of silver-plated wire of 2 mm OD having a coil length of 3 cm and radius of 1.7 cm. The measured coil inductance L_0 was 1.7 μH with a Q-factor of 120. To maintain constant mercury pressure the cold-spot temperature of the discharge was controlled and kept at 40 ± 1 °C during discharge operation over the range of power.

The voltage, current and phase shift at the primary coil were measured with the set-up described in [6] and [7] where similar electrical parameters were measured in capacitive RF discharges. A 13.56 MHz RF source was connected through an electrically symmetric matching network to the primary coil which initiated and maintained the discharge. In comparison with an asymmetric (e.g., coaxial) configuration, symmetric driving of the inductor coil reduces the RF potential between the coil ends and the plasma by a factor of two (there is a virtual ground at the centre of the coil) likewise reducing the capacitive coupling between the coil and plasma due to stray capacitive current paths through the glass. The small physical contact area between the coil and the glass also limits the capacitive coupling between the coil and ground.

The voltage was measured directly across the primary coil through a voltage divider and the current was measured with a current transformer. The measurement accuracy of voltage and current was within $\pm 5\%$. The relative phase shift between the voltage and current was measured using a vector voltmeter with accuracy $\pm 0.2°$.

The measured primary voltage V_1, current I_1 and power factor $\cos\varphi$ are shown in figures 5 and 6 as functions of total power P. The total primary resistance

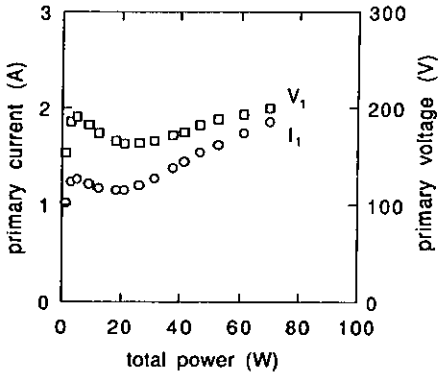

Figure 5. The current and voltage on the primary coil versus total RF power.

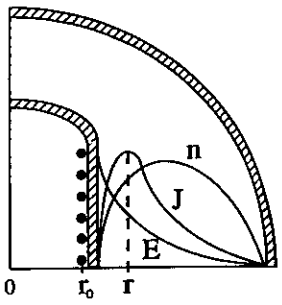

Figure 4. An axisymmetric view of partial cross section of the experimental configuration is shown here along with a qualitative diagram of the radial distribution of the RF field E, the plasma density n_e and the discharge current density J. The coil radius is r_0 and the effective discharge radius is r.

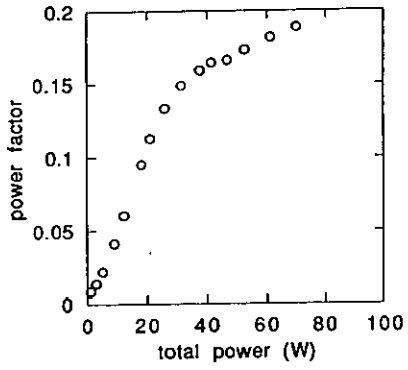

Figure 6. The phase shift between voltage and current in the primary coil versus total RF power.

DOCKET ALARM

Explore Litigation Insights

Docket Alarm provides insights to develop a more informed litigation strategy and the peace of mind of knowing you're on top of things.

Real-Time Litigation Alerts

Keep your litigation team up-to-date with **real-time alerts** and advanced team management tools built for the enterprise, all while greatly reducing PACER spend.

Our comprehensive service means we can handle Federal, State, and Administrative courts across the country.

Advanced Docket Research

With over 230 million records, Docket Alarm's cloud-native docket research platform finds what other services can't. Coverage includes Federal, State, plus PTAB, TTAB, ITC and NLRB decisions, all in one place.

Identify arguments that have been successful in the past with full text, pinpoint searching. Link to case law cited within any court document via Fastcase.

Analytics At Your Fingertips

Learn what happened the last time a particular judge, opposing counsel or company faced cases similar to yours.

Advanced out-of-the-box PTAB and TTAB analytics are always at your fingertips.

API

Docket Alarm offers a powerful API (application programming interface) to developers that want to integrate case filings into their apps.

LAW FIRMS
Build custom dashboards for your attorneys and clients with live data direct from the court.

Automate many repetitive legal tasks like conflict checks, document management, and marketing.

FINANCIAL INSTITUTIONS
Litigation and bankruptcy checks for companies and debtors.

E-DISCOVERY AND LEGAL VENDORS
Sync your system to PACER to automate legal marketing.